Supplementary Information: Direct observation of a roaming intermediate and its dynamics

Grite L. Abma,[1] Michael A. Parkes,[2] Weronika O. Razmus,[3] Yu Zhang,[4] Adam S. Wyatt,[4] Emma Springate,[4] Richard T. Chapman,[4] Daniel A. Horke,[1*], Russell S. Minns[3*]

[1]Radboud University, Institute for Molecules and Materials, Heijendaalseweg 135, 6525 AJ Nijmegen, The Netherlands

[2]Department of Chemistry, University College London, 20 Gordon Street, London

[3]School of Chemistry, University of Southampton, Highfield, Southampton SO17 1BJ, UK

[4]Central Laser Facility, STFC Rutherford Appleton Laboratory, Didcot, Oxfordshire OX11 0QX, UK

[*]To whom correspondence should be addressed; DAH: d.horke@science.ru.nl, RSM: r.s.minns@soton.ac.uk.

Experimental Details

A detailed experimental setup has been published before, and only a brief overview is given here. (*Smith et al.(2018)Smith, Warne, Bellshaw, Horke, Tudorovskya, Springate, Jones, Cacho, Chapman, Kirrander, and Minns*) 1.5 bar of 2% acetaldehyde in helium (BOC speciality gases) is expanded into a molecular beam using a piezovalve operating at 1 kHz repetition rate. The produced molecular beam is skimmed once before entering the interaction chamber, where it is intersected by the pump and probe laser pulses. Produced photoelectrons are detected using an electron time-of-flight spectrometer (Kaesdorf ETF11).

Pump and probe laser pulses are derived from an amplified Ti:Sapphire laser system, operating at 1 kHz repetition rate (Red Dragon, KM Labs). The dispersion can be independently controlled in both beams using individual grating compressors. The pump beam at 262 nm is generated via subsequent second and third harmonic generation in beta-barium borate (BBO) crystals, which typically yielded 60 fs duration pulses at 10 uJ pulse energy. XUV probe pulses were generated via high-harmonic generation in an Argon gas-jet, driven by the second harmonic of the fundamental. The seventh harmonic of the drive laser (22.3 eV) is subsequently selected using a time-preserving monochromator (*Frassetto et al.(2011)Frassetto, Cacho, Froud, Turcu, Villoresi, Bryan, Springate, and Poletto*), yielding 30 fs duration pulses with a typical flux of 10^{10} ph/s and a bandwidth of 130 meV (as detailed below). Pump and probe laser pulses are independently focused and then overlapped at a shallow angle (3 degrees) at the interaction point of the electron spectrometer.

XUV bandwidth

The bandwidth of the XUV probe pulses was evaluated from the photoelectron spectrum of atomic Xenon, shown in Figure 1. The observed lines (corresponding to the $5p_{3/2}$ and $5p_{1/2}$ final states) were fitted with a Gaussian function, yielding bandwidth (FWHM) of 135 meV

29 ($5p_{3/2}$) and 128 meV ($5p_{1/2}$).

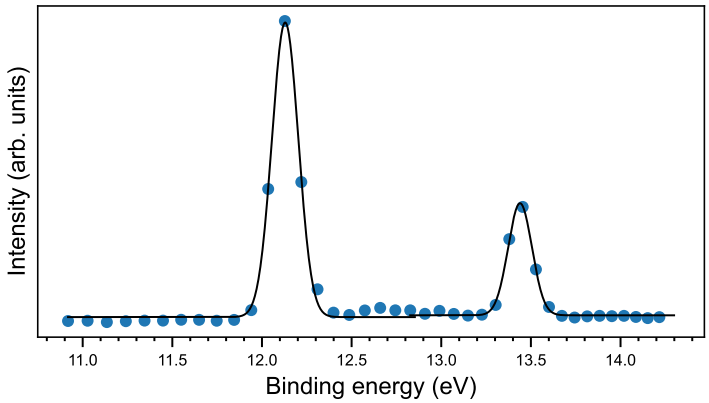

Figure 1: Photoelectron spectrum of atomic Xenon, with Gaussian fits to determine the harmonic bandwidth.

30 Photoelectron energy calibration

31 The energy of detected photoelectrons is calibrated by comparison with a published single-
32 photon photoelectron spectrum for acetaldehyde (*Bieri et al.(1982)Bieri, Åsbrink, and von*
33 *Niessen*). A direct comparison between our data and previously published data is shown in Fig-
34 ure 2.

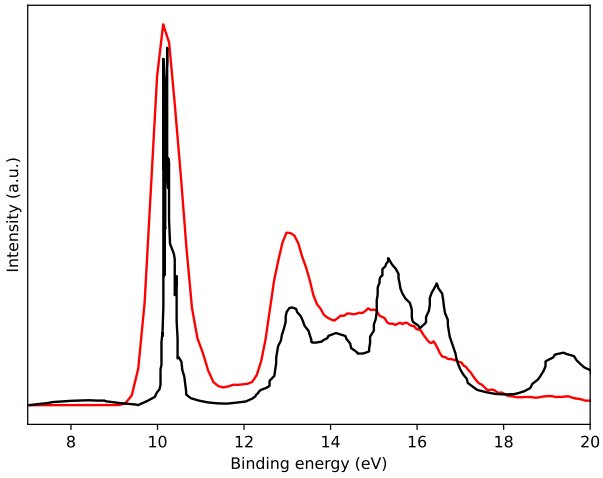

Figure 2: Overlay of the photoelectron spectrum measured using femtosecond XUV pulses (red trace) on an experimental He(II) photoelectron spectrum. (*Bieri et al.(1982)Bieri, Åsbrink, and von Niessen*) (black trace)

Data Analysis

Raw photoelectron spectra

The raw (non background subtracted) photoelectron spectra are shown in Figure 3 (on a logarithmic intensity scale) for three selected pump-probe delays. This clearly shows the relatively small excited-state signal compared to the ground state non-pumped signal, which arises from a combination of low excitation fraction and potentially lower ionisation cross-section of the excited state. For binding energies above ~ 9 eV any excited state (or product) signal is hidden within the large ground-state feature.

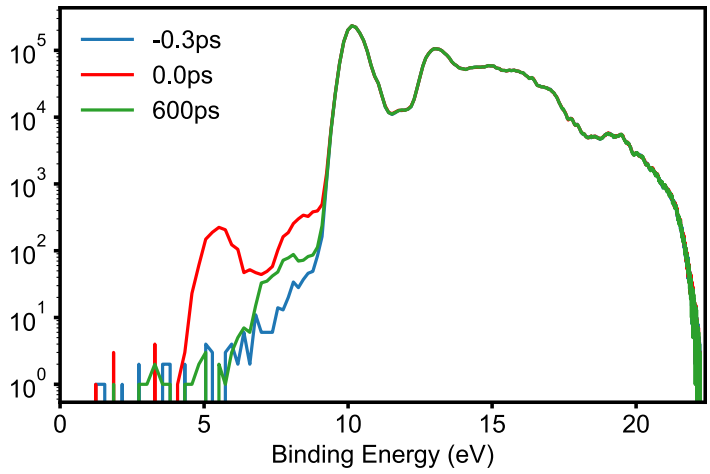

Figure 3: Photoelectron spectra of acetaldehyde for selected pump-probe delays.

Energy-integrated time-resolved plots

Figure 2 in the main paper shows the photoelectron intensity as a function of pump-probe delays integrated over 2 different photoelectron energy ranges. Statistical error bars for these data were evaluated by splitting the total collected dataset of 3141 experimental cycles into batches of 20 cyles, and evaluating the standard error on the collected photoelectron spectra. This error was then propagated to yield the shown error bars for energy-integrated traces.

Decay associated spectra

To deconvolve the various contributions to the spectrum we performed a 2D global least-squares fit to the data. The procedure simultaneously fits all photoelectron kinetic energies, ϵ_k, and time delays, t, to a function of the form

$$S(\epsilon_k, t) = g(t) \circledast \sum_{n=1}^{n} D_i(\epsilon_k) e^{-t/\tau}. \quad (1)$$

The fitting procedure assumes that the various configurations of the molecule produce a spectrum that is discrete and does not change in time. Within this assumption the fit then finds the shape of the spectrum associated with each component and how their relative contributions to the overall spectrum changes over the course of the measurement. In equation 1, $D_i(\epsilon_k)$ represents the so called decay associated spectra (DAS) that provide the energy dependent amplitudes for each of the contributing components to the overall spectrum. These are convolved with a Gaussian, $g(t)$, that represents the instrument response function and multiplied by an exponential decay, $e^{-t/\tau}$ that describes how the intensity of the DAS changes with time. The fit is performed with the minimum number of terms in the sum required to obtain a good fit such that no systematic differences are observed in plots of the residual error. Here we required three separate time constants to accurately represent the experimental data. The DAS fitting furthermore yielded an instrument response function (corresponding to the pump-probe cross-correlation) of 124 fs (FWHM).

The reconstructed 2D time-resolved photoelectron spectrum is shown in Figure 4, along with three spectra at selected time delays. For comparison, the experimental spectra at theose time delalys are shown as dashed lines. A very good match between the DAS fitting routine and experimental data is achieved, confirmed by the residual surface shown in Figure 5.

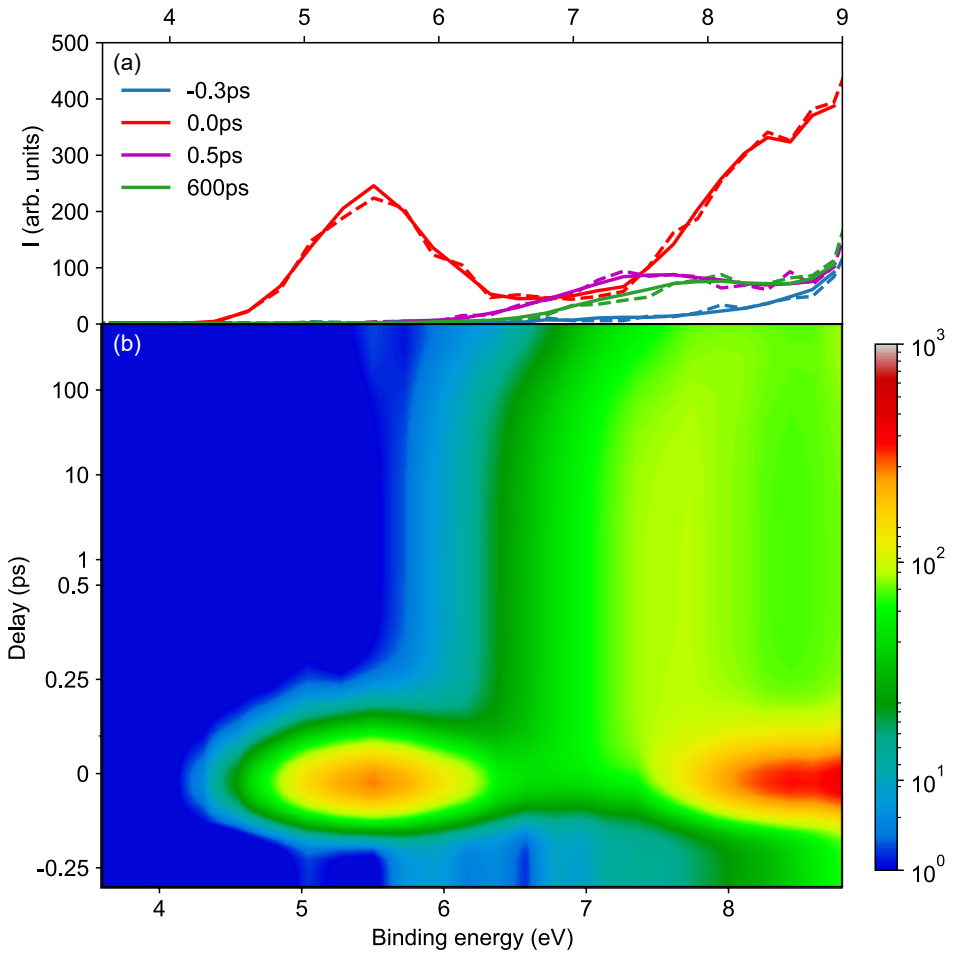

Figure 4: Results of the DAS fitting. (a) Extracted photoelectron spectra at four representative time delays extracted from the DAS fit (solid lines), and corresponding experimental spectra (dashed lines) for comparison. (b) The full 2D surface reconstructed by the DAS fit plotted on a mixed linear and logarithmic scale in time.

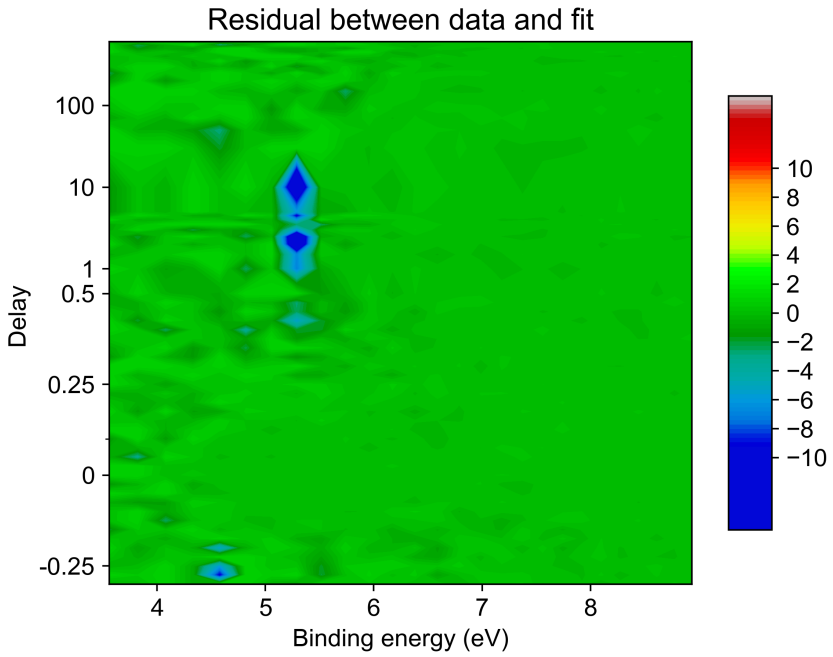

Figure 5: Residual surface comparing the DAS reconstructed 2D surfaces to the experimental data, difference given in percentage.

Computational

The vibrational frequencies and ground state structure of acetaldehyde were found by optimisation using the complete active space (CAS) self-consistent field method as implemented in the MolPro package. (*Werner et al.(2015)Werner, Knowles, Knizia, Manby, Schütz, Celani, Györffy, Kats, Korona, Lindh, Mitrushenkov, Rauhut, Shamasundar, Adler, Amos, Bernhardsson, Berning, Cooper, Deegan, Dobbyn, Eckert, Goll, Hampel, Hesselmann, Hetzer, Hrenar, Jansen, Köppl, Liu, Lloyd, Mata, May, McNicholas, Meyer, Mura, Nicklass, O'Neill, Palmieri, Peng, Pflüger, Pitzer, Reiher, Shiozaki, Stoll, Stone, Tarroni, Thorsteinsson, and Wang*) The 6-311G** basis was used and the active space had 14 electrons and 13 orbitals. The orbitals included in the active space are shown in Figure 6. The ground state structure is shown in Table 1, while vibrational frequencies and their symmetries are given in Table 2.

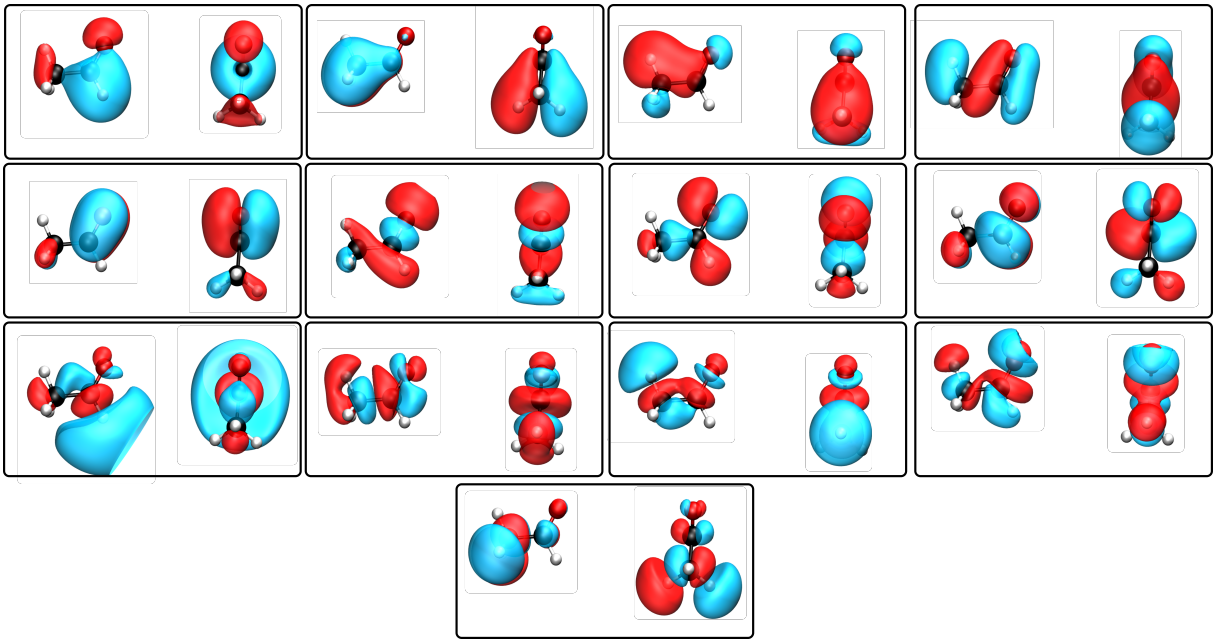

Figure 6: Molecular orbitals included in the CAS space.

Using the CAS ground state equilibrium structure state averaged CAS calculations were

Atom	X /Å	Y /Å	Z /Å
O	-1.22396	0.366606	0
C	0.938853	-0.69637	0
C	-0.01404	0.468035	0
H	1.597243	-0.64969	0.891176
H	0.385637	-1.65162	0
H	1.597243	-0.64969	-0.89118
H	0.460675	1.459567	0

Table 1: Calculated ground state structure of acetaldehyde from a CAS calculation using the 6-311G** basis set.

performed to examine the excited states of acetaldehyde. Initially 4 states were included in the state-averaged CAS calculation. But the energetic separation of the third and fourth states from the first two states was around 4 eV and examination of the surfaces showed that they did not come closer in energy. Therefore, we only included two states in the state-averaged CAS for further calculations. The A‘ ground state (S_0) and the A” first excited state (S_1). Figure 7 shows a comparison of the calculated adiabatic energy between S_0 and S_1 and the experimental photoabsorption spectrum. (*Keller-Rudek et al.(2013)Keller-Rudek, Moortgat, Sander, and Sörensen*) The calculated energy of S_1 relative to S_0 is 4.52 eV. As is clear the agreement between the calculated and measured transition energy is good.

Potential energy scans were performed to examine the S_0 and S_1 potential energy surfaces. Two types of scans were made. In the first a fixed scan was performed where all structural parameters were fixed apart from the C-C bond between the CH_3 and COH moieties and the C-O-H angle. Relaxed scans were also performed along the C-C bond. The relaxed scans were performed minimising either the energy of the S_0 or the S_1 states. The results of these scans are shown in Figure 8. From these scans key points on the potential energy surface were chosen for further calculations to be performed of ionization propensity. For these calculations the EOM-IP-CCSD method in Q-CHEM was used (*Shao et al.(2015)Shao, Gan, Epifanovsky, Gilbert, Wormit, Kussmann, Lange, Behn, Deng, Feng, Ghosh, Goldey, Horn, Jacobson, Kaliman, Khal-*

Mode Number	Symmetry	Frequency / cm^{-}1
1	A”	155.36
2	A’	525.91
3	A”	820.37
4	A’	931.46
5	A’	1179.14
6	A”	1188.22
7	A’	1429.48
8	A’	1485.37
9	A”	1496.80
10	A’	1511.40
11	A’	1808.73
12	A’	2934.89
13	A”	2995.83
14	A’	3041.38
15	A’	3061.97

Table 2: Ground state frequencies of acetaldehyde from a CAS calculation using the 6-311G** basis set

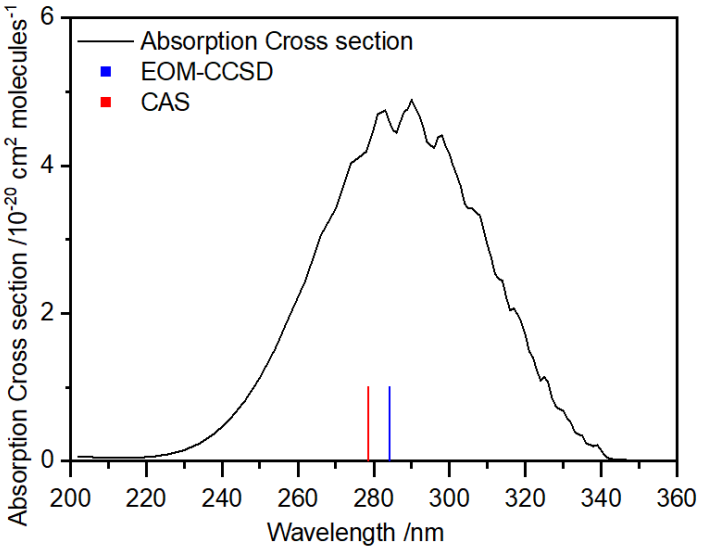

Figure 7: Comparison of experimental photoabsorption spectrum to calculated band positions using SA-CAS (14,13) and EOM-CCSD with the 6-311G** basis set. Experimental spectrum is taken from (*Keller-Rudek et al.(2013)Keller-Rudek, Moortgat, Sander, and Sörensen*)

iullin, Kuś, Landau, Liu, Proynov, Rhee, Richard, Rohrdanz, Steele, Sundstrom, Woodcock, Zimmerman, Zuev, Albrecht, Alguire, Austin, Beran, Bernard, Berquist, Brandhorst, Bravaya, Brown, Casanova, Chang, Chen, Chien, Closser, Crittenden, Diedenhofen, DiStasio, Do, Dutoi, Edgar, Fatehi, Fusti-Molnar, Ghysels, Golubeva-Zadorozhnaya, Gomes, Hanson-Heine, Harbach, Hauser, Hohenstein, Holden, Jagau, Ji, Kaduk, Khistyaev, Kim, Kim, King, Klunzinger, Kosenkov, Kowalczyk, Krauter, Lao, Laurent, Lawler, Levchenko, Lin, Liu, Livshits, Lochan, Luenser, Manohar, Manzer, Mao, Mardirossian, Marenich, Maurer, Mayhall, Neuscamman, Oana, Olivares-Amaya, O'Neill, Parkhill, Perrine, Peverati, Prociuk, Rehn, Rosta, Russ, Sharada, Sharma, Small, Sodt, Stein, Stück, Su, Thom, Tsuchimochi, Vanovschi, Vogt, Vydrov, Wang, Watson, Wenzel, White, Williams, Yang, Yeganeh, Yost, You, Zhang, Zhang, Zhao, Brooks, Chan, Chipman, Cramer, Goddard, Gordon, Hehre, Klamt, Schaefer, Schmidt, Sherrill, Truhlar, Warshel, Xu, Aspuru-Guzik, Baer, Bell, Besley, Chai, Dreuw, Dunietz, Furlani, Gwaltney, Hsu, Jung, Kong, Lambrecht, Liang, Ochsenfeld, Rassolov, Slipchenko, Subotnik, Van Voorhis, Herbert, Krylov, Gill, and Head-Gordon). The calculated energy of S_1 using the EOM-CCSD method with the 6-311G** basis is shown in Figure 7 along with the value calculated using the CAS method. It can be seen that the EOM-CCSD result is in agreement with the CAS result, giving us confidence that (at least near the equilibrium structure) EOM-CCSD gives a good representation of the potential energy surface.

To test the reliability of the EOM-IP-CCSD method on our system, calculations were performed on ionization of ground state acetaldehyde and the CO and CH_3 products. Figure 9 shows the results for acetaldehyde plotted against the experimental He(II) photoelectron spectrum of Bieri *et al* (*Bieri et al.(1982)Bieri, Åsbrink, and von Niessen*). In Table 3 ionisation energies for the first three cation states of acetaldehyde, CH_3 and HCO are given with the experimental values. The experimental values for acetaldehyde are from Bieri *et al* (*Bieri et al.(1982)Bieri, Åsbrink, and von Niessen*), while those for CH_3 and HCO are from the NIST

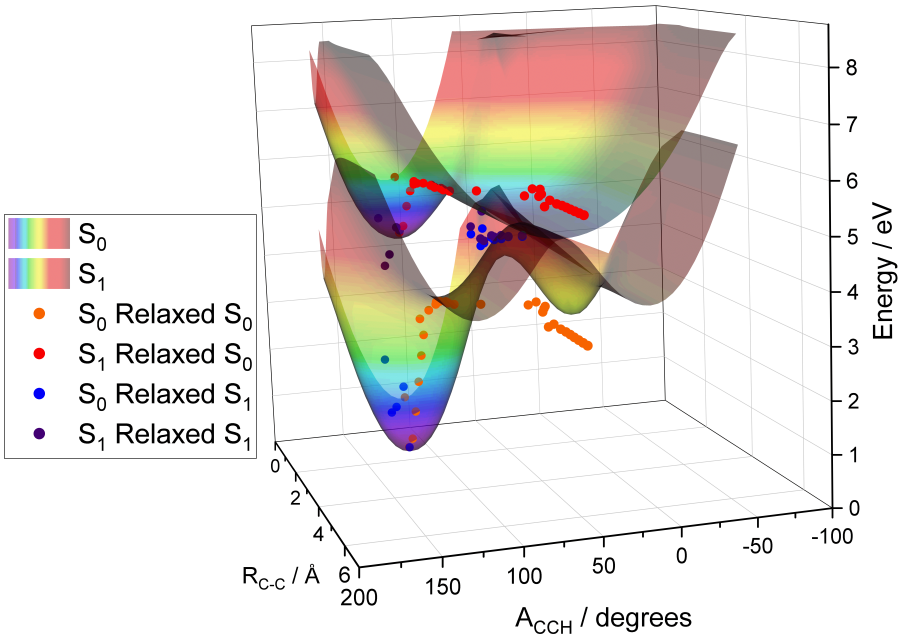

Figure 8: Potential energy surfaces of S_0 and S_1 of acetalaldhyde calculated using SA-CAS(14:13) and the 6-311G** basis set. Full surfaces are fixed scans, points represent the energies from relaxed scans. The orange and red dots are where the S_0 state is used as the basis of the optimisation, the blue and purple are where the S_1 state is the basis

Chemistry Webbook (*Lias(2022)*). As is clear there is good agreement between experiment and theory. There is a small shift of around 0.3 eV between the calculated and experimental position of the D_0 band of the spectrum while agreement is better for the higher-lying cation states.

For all the aceetaldehyde geometries indicated on Figure 10 (S_0 and S_1 PES) the energies of the S_0, S_1, D_0 and D_1 states and the Dyson orbitals for the transitions were calculated using the EOM-IP-CCSD method with a 6-311G** basis. These orbitals were then used a input for calculation of the ionisation cross-sections using ezDyson (*Gozem and Krylov(2022)Gozem, and Krylov, Gozem et al.(2015)Gozem, Gunina, Ichino, Osborn, Stanton, and Krylov*). The results of the calculations are then presented in Figure 11 where the differences between ionisation from the two electronic states are clear.

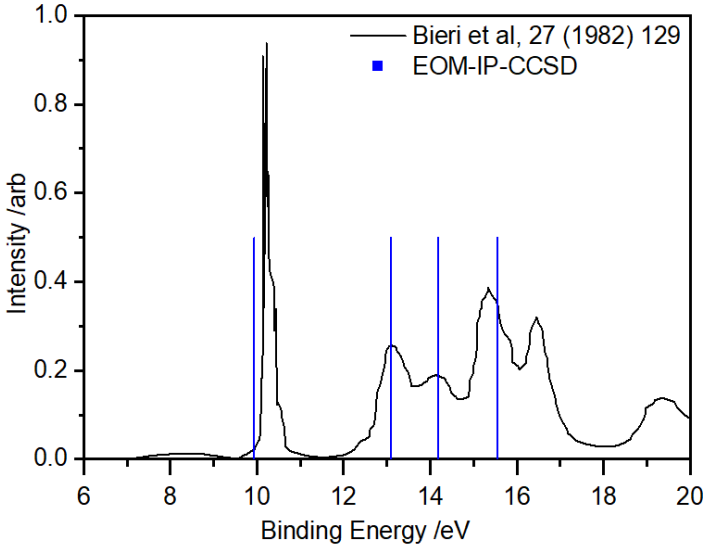

Figure 9: Comparison of experimental He(II) photoelectron spectrum to calculated binding energies using EOM-IP-CCSD. (*Bieri et al.(1982)Bieri, Åsbrink, and von Niessen*)

	EOM-IP-CCSD / eV	Expt / eV
Acetaldehyde D_0	9.93	10.22
Acetaldehyde D_1	13.09	13.05
Aceetaldehyde D_2	14.18	14.15
CH_3	9.55	9.84
HCO	8.97	8.12

Table 3: Comparison of experimental and calculated ionization energies

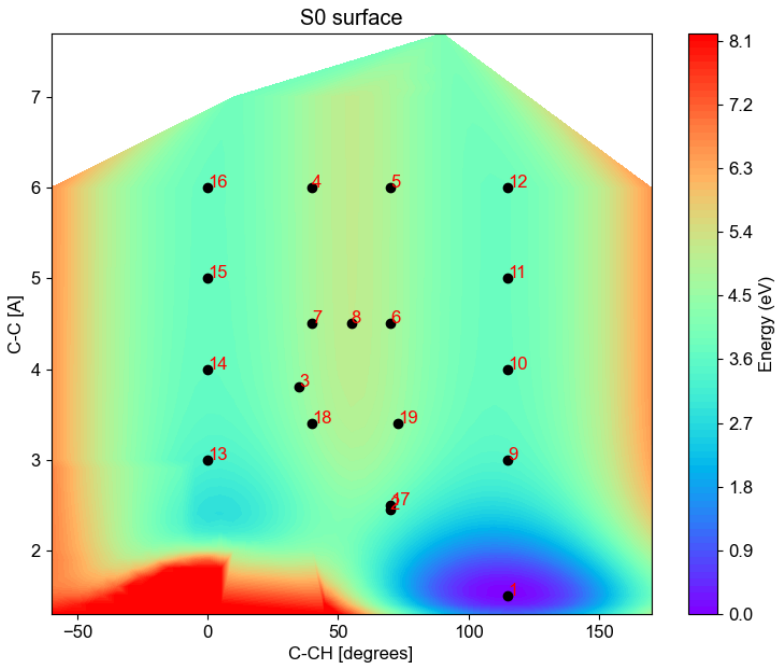

Figure 10: The calculated S0 surface with the points at which the dyson calculations were performed drawn in.

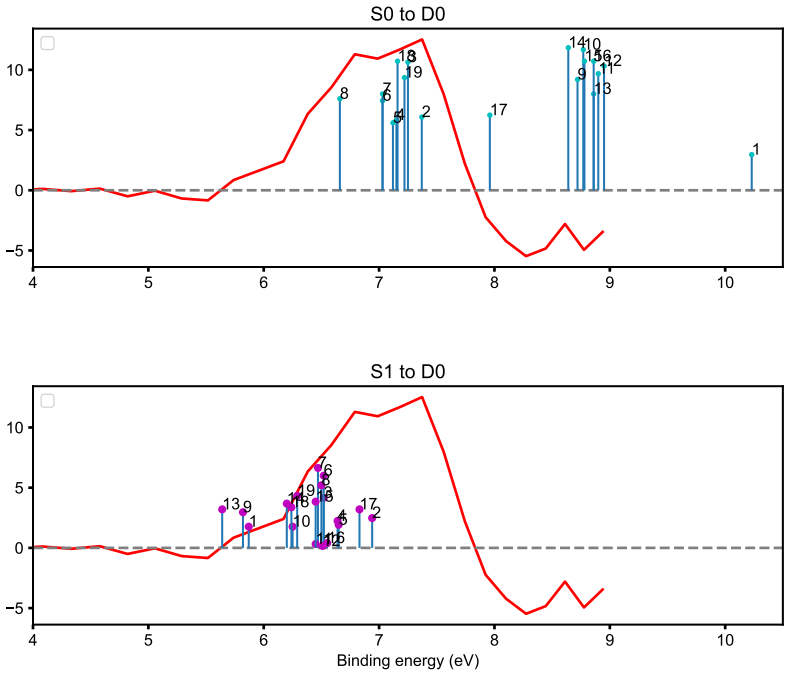

Figure 11: The energies of all calculated points on the S_0 and S_1 surface, with the number indicating to which point on the surface the energy corresponds. The length of the stick corresponds to the cross section of this transition.

References

Smith et al.(2018)Smith, Warne, Bellshaw, Horke, Tudorovskya, Springate, Jones, Cacho, Chapman, Kirrander, Smith, A. D.; Warne, E. M.; Bellshaw, D.; Horke, D. A.; Tudorovskya, M.; Springate, E.; Jones, A. J. H.; Cacho, C.; Chapman, R. T.; Kirrander, A.; Minns, R. S. Mapping the Complete Reaction Path of a Complex Photochemical Reaction. *Phys. Rev. Lett.* **2018**, *120*, 183003.

Frassetto et al.(2011)Frassetto, Cacho, Froud, Turcu, Villoresi, Bryan, Springate, and Poletto. Frassetto, F.; Cacho, C.; Froud, C. A.; Turcu, I. E.; Villoresi, P.; Bryan, W. A.; Springate, E.; Poletto, L. Single-grating monochromator for extreme-ultraviolet ultrashort pulses. *Opt. Express* **2011**, *19*, 19169–19181.

Bieri et al.(1982)Bieri, Åsbrink, and von Niessen. Bieri, G.; Åsbrink, L.; von Niessen, W. 30.4-Nm He (II) Photoelectron Spectra of Organic Molecules. *J. Electron. Spectros. Relat. Phenomena* **1982**, *27*, 129–178.

Werner et al.(2015)Werner, Knowles, Knizia, Manby, Schütz, Celani, Györffy, Kats, Korona, Lindh, Mitrushenk Werner, H.-J. et al. MOLPRO, version 2015.1, a package of ab initio programs. 2015.

Keller-Rudek et al.(2013)Keller-Rudek, Moortgat, Sander, and Sörensen. Keller-Rudek, H.; Moortgat, G. K.; Sander, R.; Sörensen, R. The MPI-Mainz UV/VIS Spectral Atlas of Gaseous Molecules of Atmospheric Interest. *Earth Syst. Sci. Data* **2013**, *5*, 365.

Shao et al.(2015)Shao, Gan, Epifanovsky, Gilbert, Wormit, Kussmann, Lange, Behn, Deng, Feng, Ghosh, Golde Shao, Y. et al. Advances in Molecular Quantum Chemistry Contained in the Q-Chem 4 Program Package. *Mol. Phys.* **2015**, *113*, 184–215.

Lias(2022). Lias, S. G. In *NIST Chemistry WebBook, NIST Standard Reference Database Number 69*; Linstrom, P. J., Mallard, W. G., Eds.; National Institute of Standards and Technology: Gaithersburg , MD, 2022.

Gozem and Krylov(2022)Gozem, and Krylov. Gozem, S.; Krylov, A. I. The *ezSpectra* Suite: An Easy-to-use Toolkit for Spectroscopy Modeling. *WIREs Comput Mol Sci* **2022**, *12*.

Gozem et al.(2015)Gozem, Gunina, Ichino, Osborn, Stanton, and Krylov. Gozem, S.; Gunina, A. O.; Ichino, T.; Osborn, D. L.; Stanton, J. F.; Krylov, A. I. Photoelectron Wave Function in Photoionization: Plane Wave or Coulomb Wave? *J. Phys. Chem. Lett.* **2015**, *6*, 4532–4540.